

2018-08-28

Hydraulic retention time affects bacterial community structure in an As-rich acid mine drainage (AMD) biotreatment process.

Fernandez-Rojo, L

<http://hdl.handle.net/10026.1/12356>

10.1007/s00253-018-9290-0

Applied Microbiology and Biotechnology

Springer Verlag

All content in PEARL is protected by copyright law. Author manuscripts are made available in accordance with publisher policies. Please cite only the published version using the details provided on the item record or document. In the absence of an open licence (e.g. Creative Commons), permissions for further reuse of content should be sought from the publisher or author.

1 **Hydraulic retention time affects bacterial community structure in**
2 **an As-rich acid mine drainage (AMD) biotreatment process**

3 Lidia Fernandez-Rojo¹; Corinne Casiot¹; Vincent Tardy¹; Elia Laroche¹; Pierre Le Pape²;
4 Guillaume Morin²; Catherine Joulian³; Fabienne Battaglia-Brunet³; Charlotte Braungardt⁴;
5 Angélique Desoeuvre¹; Sophie Delpoux¹; Jolanda Boisson⁵; Marina Héry¹.

6 ¹ *HydroSciences Montpellier, Univ. Montpellier-CNRS-IRD, Montpellier, France*

7 ² *Institut de Minéralogie, de Physique des Matériaux et de Cosmochimie (IMPMC), UMR*
8 *7590 CNRS-UPMC-IRD-MNHN, 4, place Jussieu, 75252 Paris cedex 05, France*

9 ³ *French Geological Survey (BRGM), Geomicrobiology and environmental monitoring unit,*
10 *3, avenue Claude Guillemin, BP 36009, 45060 Orléans Cedex 2, France*

11 ⁴ *School of Geography, Earth and Environmental Sciences (Faculty of Science &*
12 *Engineering), Plymouth University, United Kingdom*

13 ⁵ *IRH Ingénieur Conseil, Antegroup, 197 avenue de Fronton, 31200, Toulouse, France*

14

15 **Abstract**

16 Arsenic removal consecutive to biological iron oxidation and precipitation is an effective
17 process for treating As-rich acid mine drainage (AMD). We studied the effect of hydraulic
18 retention time (HRT) – from 74 to 456 min- in a bench-scale bioreactor exploiting such
19 process. The treatment efficiency was monitored during 19 days, and the final mineralogy and
20 bacterial communities of the biogenic precipitates were characterized by X-ray absorption
21 spectroscopy and high-throughput 16S rRNA gene sequencing. The percentage of Fe(II)
22 oxidation (10–47 %) and As removal (19–37 %) increased with increasing HRT. Arsenic was
23 trapped in the biogenic precipitates as As(III)-bearing schwertmannite and amorphous ferric
24 arsenate, with a decrease of As/Fe ratio with increasing HRT. The bacterial community in the
25 biogenic precipitate was dominated by Fe-oxidizing bacteria whatever the HRT. The
26 proportion of *Gallionella* and *Ferrovum* genera shifted from respectively 65 and 12 % at low
27 HRT, to 23 and 51 % at high HRT, in relation with physico-chemical changes in the treated
28 water. *aioA* genes and *Thiomonas* genus were detected at all HRT although As(III) oxidation
29 was not evidenced. To our knowledge, this is the first evidence of the role of HRT as a driver
30 of bacterial community structure in bioreactors exploiting microbial Fe(II) oxidation for
31 AMD treatment.

32 **Keywords:** iron-oxidizing bacteria, biogenic precipitate, *Gallionella*, *Ferrovum*, arsenic
33 removal, As(III) oxidation

34

35 **1. Introduction**

36 Arsenic (As) is a toxic element present in many cases in acid mine drainage (AMD) ^{1,2}. One
37 attractive, cost-effective way to treat As-rich AMD is to use the capacity of autochthonous
38 microorganisms to immobilize this metalloid while oxidizing and precipitating iron ³⁻⁵. This
39 process is occurring naturally and has been described in many AMD streams worldwide ⁶⁻⁸. It
40 represents a promising strategy to remediate these effluents in a passive way, with minimum
41 maintenance, which is a prerequisite in the management of these pollutions that last hundreds
42 of years ⁹.

43 In a recent study, we demonstrated that higher Fe(II) oxidation and As removal were obtained
44 with increasing hydraulic retention time (HRT) in a bench-scale bioreactor treating As-rich
45 AMD ¹⁰. However, the effect of HRT on the microbial community structure and mineralogy
46 of the biogenic precipitate was not investigated, although these features are major issues in
47 the development of a bioremediation process.

48 By changing the physico-chemical parameters of the water, HRT may affect the bacterial
49 community that drives the depollution and, in turn, treatment performance, robustness or
50 sustainability, as observed in AMD treatments exploiting microbial sulfate reduction ^{11,12}. A
51 number of studies have highlighted the role of pH ¹³⁻¹⁵, conductivity ¹⁶ or oxygen
52 concentration ¹⁷ in the structuration of microbial communities in AMD.

53 HRT is also expected to influence the As and Fe contents of the precipitate and, in turn, the
54 mineralogy of As-bearing phases; the latter controls the concentration of aqueous As species
55 in equilibrium with the solid and the potential reversibility of As trapping towards physico-
56 chemical changes or ageing ¹⁸.

57 In the present study, we investigated the effect of HRT on the composition of the bacterial
58 community and the mineralogy of the biogenic precipitate in a bench-scale Fe-oxidation
59 bioreactor treating As-rich AMD from the Carnoulès mine (southern France).

60 **2. Materials and methods**

61 **2.1. Bench-scale aerobic bioreactor**

62 The current bioreactor has been described in detail in our previous study ¹⁰. Briefly, the
63 bioreactor comprises four polyvinyl chloride (PVC) channels (C1–C4) of 1 m length, 0.06 m
64 width and 0.06 m depth. A biodegradable mesh (BIO DURACOVER) was placed inside the
65 channels to favor the adhesion of the biogenic precipitate. A peristaltic pump (Gilson,
66 Minipuls 3) transferred AMD from a tank to the four channel inlets. Another pump was used
67 to maintain the water height at 4 mm. Each channel was fitted with a specific peristaltic pump
68 tubing (Tygon[®] internal diameter (i.d.) 3.17, 1.65, 1.00 and 0.76 mm), thus setting a different
69 flow rate value (3.94, 1.34, 0.68 and 0.41 mL min⁻¹, respectively) and hydraulic retention time
70 (HRT = 74, 130, 200 and 456 min, respectively). The studied HRT values were chosen in a
71 way they cover a range of iron oxidation efficiency from ~10 % to ~90 %, according to our
72 previous study ¹⁰. Conditions of temperature and light were set up as previously described ¹⁰.

73

74 **2.2. Experimental design**

75 Water was collected (~200 L) from the spring of the Reigous Creek on June 2nd of 2015 in
76 20 L containers previously decontaminated with 65 % HNO₃ and rinsed three times with *in*
77 *situ* AMD. Once returned to the laboratory, the containers were purged with N₂ until

78 dissolved oxygen (DO) was lower than $\sim 1 \text{ mg L}^{-1}$, in order to avoid Fe(II) oxidation. The
79 containers were stored and successively used as feed water throughout the duration of the
80 experiment. The experiment started on June 3rd of 2015, running in the four bioreactor
81 channels (C) in parallel, each with a fixed HRT that was maintained throughout the
82 experiment. Hence, the total volume of treated water at the end of the experiment varied from
83 one channel to the other (~ 105 to 10 L), depending on the flow rate.

84 During the initial setting-up stage of the experiment, a steady-state condition regarding Fe(II)
85 oxidation within the channel was reached within 8 days. During that time, Fe precipitation
86 promoted the formation of orange biogenic precipitates that covered the bottom of the
87 channels¹⁰. Once the steady-state was reached, the efficiency of the treatment in terms of Fe
88 oxidation, Fe precipitation and As removal, was evaluated for each channel, *i.e.* hydraulic
89 retention time. The associated rates (in $\text{mol L}^{-1} \text{ s}^{-1}$) were calculated using Equation 1,

$$\text{Rate} = \frac{([X]_{inlet} - [X]_{outlet})}{HRT} \quad \text{Equation 1}$$

90 where [X] was the concentration of dissolved Fe(II), total dissolved Fe, total dissolved As,
91 dissolved As(III) or dissolved As(V), respectively, in mol L^{-1} . The exact HRT was calculated
92 by dividing the experimental volume of water recovered from one channel by the flow rate (in
93 mL min^{-1}) measured at the channel inlet.

94 Nineteen days after the start of the experiment, the water was removed from the channels. The
95 biogenic precipitates were recovered by scraping the biodegradable mesh with a sterilized
96 spatula. The biogenic precipitate that covered the first section of the channel bottom (0–50
97 cm, closest to inlet) was separated from that in the second section (50–100 cm, closest to

98 outlet). The biogenic precipitates were collected into Falcon Tubes (50 mL) and centrifuged
99 for 10 min at $4400 \times g$ (Sorwall ST40, Thermo Scientific). Sample from the first section
100 (referred as Channel No X-1st section, abbreviated as CX-1st) was distributed into six aliquots:
101 three for bacterial cell quantification, one for bacterial community analysis and *aioA* gene
102 quantification, one for As redox speciation and one for mineralogy determination. The second
103 section (abbreviated as CX-2nd) yielded less biogenic precipitates and was distributed in two
104 aliquots only, one for As redox speciation and one for the mineralogy analysis.

105 **2.3. Experimental monitoring**

106 **2.3.1. Chemical analyses**

107 Water samples were collected every third day at the channel inlets and outlets to monitor the
108 main physico-chemical parameters (DO, temperature, pH, conductivity and redox potential)
109 and the rate of Fe(II) oxidation, together with Fe and As removal within the channels.
110 Samples were filtered (0.22 μm) and analyzed for dissolved Fe(II) by spectrophotometry, total
111 dissolved Fe and As by ICP-MS (inductively coupled plasma-mass spectrometer), and As
112 speciation by HPLC-ICP-MS (high performance liquid chromatography-ICP-MS). The
113 biogenic precipitate was analyzed for total As and Fe content by ICP-MS after acid digestion
114 with aqua regia. Details of these analytical procedures are reported in Fernandez-Rojo *et al.*¹⁰
115 and in its supporting information file.

116 **2.3.2. Microbiological analyses**

117 Bacterial cell counting, DNA extraction and quantification of 16S rRNA genes and *aioA*
118 genes were performed on the Reigous Creek original water used to feed the bioreactor, and on
119 the biogenic precipitates (1st section) recovered at the bottom of each channel at the end of the

120 experiment, as described previously¹⁰. All DNA extractions were performed on triplicates.
121 DNA extracts were quantified with a fluorometer (Qubit[®], Invitrogen) and stored at -20 °C
122 until further analysis.

123 The diversity and taxonomic composition of the bacterial communities of water and biogenic
124 precipitates samples were determined by Illumina high-throughput sequencing of bacterial
125 16S rRNA genes. V4-V5 region (about 450 bases) was amplified by PCR using primers
126 PCR1_515F¹⁹ and PCR1_928R²⁰. The PCR products were sent to GeT-PlaGe platform
127 (Toulouse, France) for Illumina MiSeq analysis using a 2 × 300 bp protocol. Bioinformatics
128 analyses of 16S rRNA gene sequences were performed with MOTHUR version 1.31²¹.
129 Taxonomic affiliation was performed with a Bayesian classifier²² (using a 80 % bootstrap
130 confidence score) against the SILVA reference database v128. To homogenize the datasets
131 the number of reads per sample was reduced to the lowest dataset by random selection
132 (26 000 reads). High quality sequences were then selected and clustered into operational
133 taxonomic units (OTUs) using a 97% cut-off. Diversity indices, rarefaction curves were
134 calculated with MOTHUR at a level of 97 % sequence similarity. The raw datasets are
135 available on the EBI database system under project accession number [...]). Details of these
136 analytical procedures are reported in Tardy *et al.*²³

137 **2.3.3. Mineralogy and As speciation analyses**

138 Samples of the biogenic precipitates were kept under anaerobic conditions and dried under
139 vacuum at room temperature. The As-bearing phases and the As redox state were determined
140 by EXAFS (extended X-ray absorption fine structure) and XANES (X-ray absorption near
141 edge structure), respectively, at the As K-edge. The Fe-bearing phases were determined only
142 in C1 and C4 (1st and 2nd section) by EXAFS at the Fe K-edge. The As and Fe K-edge

143 EXAFS and XANES spectra were collected at 80 K in transmission mode on the XAFS
144 beamline (ELETTRA, Trieste, Italy). Two scans were averaged for each sample, normalized
145 and background subtracted over the 0–15 Å⁻¹ *k*-range for As and over the 0–17 Å⁻¹ *k*-range
146 for Fe using the Athena Software ²⁴. Linear combination fitting (LCF) of the *k*³-weighted
147 EXAFS data was performed over the 3–15 Å⁻¹ *k*-range for As and the 2–17 Å⁻¹ *k*-range for
148 Fe, with the same software. Detailed procedures are described in Fernandez-Rojo *et al.* ¹⁰ and
149 its supporting information file. LCF analysis of the XANES data was performed by Resongles
150 *et al.* ²⁵ using an in-house program based on a Levenberg–Marquardt algorithm. As(III) and
151 As(V) coprecipitated schwertmannites ²⁶ were used as model compounds.

152 **2.3.4. Statistical analyses**

153 The non-parametric Kruskal-Wallis test was used with a significance level of 0.05 in order to
154 test whether Fe oxidation, Fe precipitation, As removal, bacterial cell concentration and
155 *aioA*/16S gene ratio were statistically different between the four HRT. If the p-value of the
156 Kruskal-Wallis test was lower than 0.05, Dunn’s multiple comparison tests with Bonferroni p-
157 value adjustment were performed. Differences in bacterial composition between C1-74 min
158 and C4-456 min were compared by one-way ANOVA, with a significance level of 0.05. The
159 statistical analyses were performed with the R free software (<http://www.r-project.org/>).

160 **3. Results**

161 **3.1. Treatment efficiency**

162 The mean chemical composition of the feed water at the inlet of each channel exhibited the
163 typical characteristics of the Reigous Creek AMD ^{7,27}. The pH averaged 3.65, total dissolved

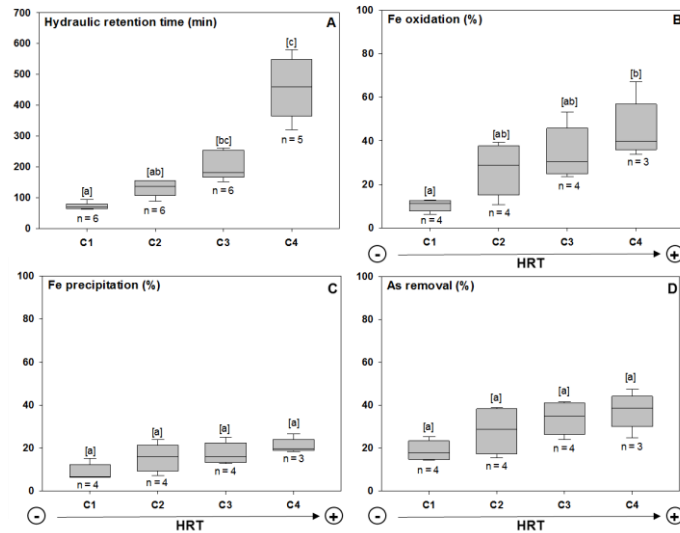
164 Fe concentration averaged 480 mg L^{-1} (~95 % Fe(II)) and total dissolved As concentration
165 averaged 35 mg L^{-1} (~17 % As(V)) (Table S1). The physico-chemical parameters and total
166 dissolved Fe and As concentrations did not vary as much as 4% between the four channel
167 inlets (Table S1), despite important difference in DO concentration (from 4 to 7 mg L^{-1}).
168 During the course of the experiment, inlet water parameters varied generally by less than
169 10%, except DO and total dissolved As concentrations (36-42 %). The latter continuously
170 decreased throughout experiment duration, due to precipitation in the feed tank, which equally
171 impacted the four channel inlets.

172 Fe oxidation, Fe precipitation and As removal showed an upward trend with increasing HRT
173 (Figure 1A); iron oxidation ranged from 10 % in C1-74 min to 47 % in C4-456 min (Figure
174 1B), Fe precipitation ranged from 9 % in C1 to 22 % in C4 (Figure 1C), and As removal
175 ranged from 14 % in C1 to 48 % in C4 (Figure 1D). Efficiency was subjected to some
176 temporal variation, as evidenced by dispersion of data in each boxplot. This could be related
177 to the difficulty in maintaining a constant hydraulic retention time.

178 The outlet water chemistry varied accordingly to Fe oxidation, Fe precipitation and As
179 removal between the channels (Figure 2). The most noteworthy changes from C1-74 to C4-
180 456 min were associated to pH decrease, from 3.2 to 2.8, dissolved Fe(II) concentration
181 decrease (from 400 to 240 mg L^{-1}), dissolved Fe(III) increase (from 30 to 120 mg L^{-1}), and
182 dissolved arsenic concentration (both As(III) and As(V)) decrease, from 25 to 15 mg L^{-1}
183 (Figure 2).

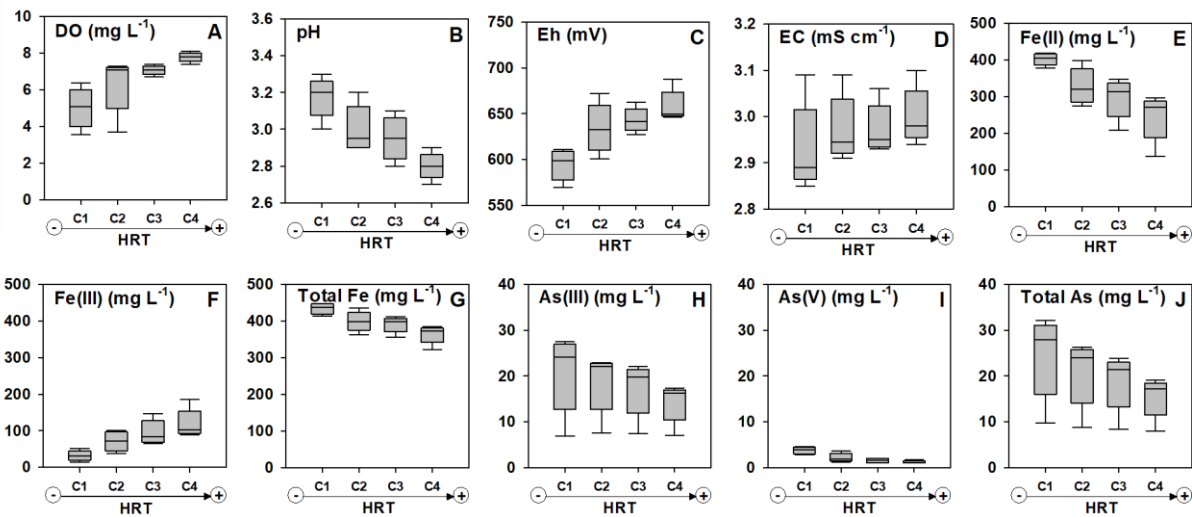
184

185



186 **Figure 1.** Boxplot representations of the HRT maintained on each channel for the whole duration of the
 187 experiment (A), and Fe oxidation (B), Fe precipitation (C) and As removal (D) at the steady-state. The vertical
 188 limits of the boxes represent the first and third quartiles and the line inside the box is the median. The extend of
 189 the whiskers shows the entire range of the data. Different letters in brackets indicate statistically significant
 190 differences between the groups (p -value < 0.05) according to Kruskal-Wallis and Dunn's multiple comparison
 191 tests. n= number of samples.

192

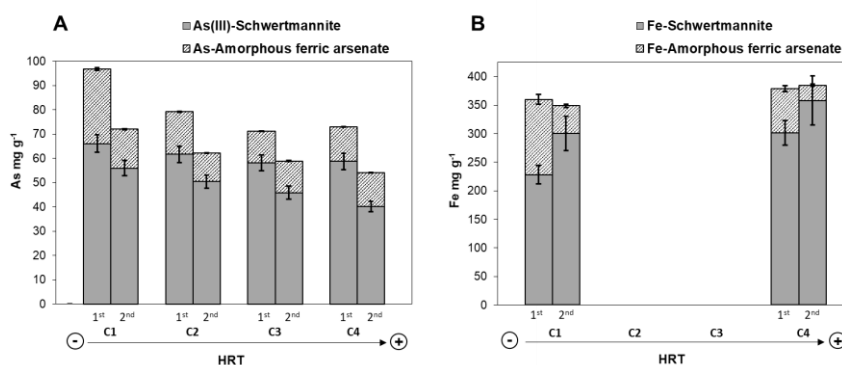


193 **Figure 2.** Boxplot representations of dissolved oxygen (DO) (A), pH (B), redox potential (Eh) (C), electrical
 194 conductivity (EC) (D), Fe(II) (E), Fe(III) (F), total Fe (G), As(III) (H), As(V) (I) and total As (J) determined in
 195 the outlet water. Representation of data as boxplots as described for Figure 1.

196 **3.2. Arsenic speciation and mineralogy of the biogenic precipitates**

197 The biogenic precipitates contained an average of $71 \pm 13 \text{ mg g}^{-1}$ of As, and $366 \pm 11 \text{ mg g}^{-1}$
198 of Fe (Table 1). The As/Fe molar ratio decreased with increasing HRT (0.2 to 0.1 from C1 to
199 C4), and from the first section to the second section of the channels (Table 1, Figure 3).

200 As-XANES LCF indicated that arsenic was mainly in the form of As(III) ($\geq 65 \%$). As-
201 EXAFS LCF showed that arsenic was mainly distributed between two distinct solid phases,
202 with little variation among samples: As(III) sorbed to schwertmannite (68 to 82 %), and
203 As(V) in amorphous ferric arsenate (18 to 32 %) (Table 1, Figure 3A). Fe-EXAFS LCF
204 indicated that iron was predominantly in schwertmannite (64 – 91%) and, to a lower extent, in
205 amorphous ferric arsenate (9 – 36%) (Figure 3B). The proportion of schwertmannite was
206 slightly higher in the second section of the channels than in the first one.



207 **Figure 3.** Arsenic (A) and iron (B) solid speciation derived from LCF analysis of EXAFS spectra collected at the
208 As and Fe K-edges on the biogenic precipitates in the 1st and 2nd section of the channels. Corresponding
209 experimental and LCF spectra are displayed in Figure S1 and Figure S2, respectively. LCF results are reported in
210 Table S2 and Table S3, respectively.

212 **Table 1.** Chemical and mineralogical composition of the biogenic precipitates recovered from the channel bottom at the end of the experiments.

| Sample | Biomass | Chemical composition from Acid Digestion | | | As oxidation state from As K-edge XANES | | As-bearing phases from As K-edge EXAFS | | Fe-bearing phases from Fe K-edge EXAFS | |
|--------------------|--|--|--------------------------------|--------------------------------|--|------------------------------|---|------------------|---|------------|
| | cells g ⁻¹ (dry wt.) × 10 ⁷ | Total As mg g ⁻¹ | Total Fe mg g ⁻¹ | As/Fe mol mol ⁻¹ | As(III)/As _T (%) | As(V)/As _T (%) | Schw As(III) (%) | AFA As(V) (%) | Schw (%) | AFA (%) |
| | C1-1 st | 2.4(5) | 97(5) | 356(5) | 0.20(2) | 65(2) | 35(2) | 68(2) | 32(1) | 64(5) |
| C1-2 nd | n.d. | 72(5) | 349(5) | 0.15(1) | 76(2) | 24(2) | 78(2) | 22(2) | 86(11) | 14(9) |
| C2-1 st | 1.6(2) | 79(5) | 362(5) | 0.16(2) | 76(2) | 24(2) | 78(2) | 22(2) | n.d. | n.d. |
| C2-2 nd | n.d. | 62(5) | 371(5) | 0.13(1) | 80(2) | 20(2) | 81(2) | 19(1) | n.d. | n.d. |
| C3-1 st | 1.6(5) | 71(5) | 364(5) | 0.15(1) | 79(2) | 21(2) | 82(3) | 18(2) | n.d. | n.d. |
| C3-2 nd | n.d. | 59(5) | 365(5) | 0.12(1) | 77(2) | 23(2) | 78(3) | 22(2) | n.d. | n.d. |
| C4-1 st | 3.9(2) | 73(5) | 379(5) | 0.14(1) | 79(2) | 21(2) | 80(3) | 20(2) | 82(5) | 18(5) |
| C4-2 nd | n.d. | 54(5) | 385(5) | 0.10(1) | 73(2) | 27(2) | 74(2) | 26(1) | 92(11) | 8(9) |

213 n.d. = not determined

214 As K-edge XANES LCF results are from Resongles et al.²³ (see equivalence of sample names in Table S4). As K-edge EXAFS LCF were performed using As(III)-sorbed
 215 schwertmannite (Schw As(III)) and Amorphous Ferric Arsenate (AFA) as fitting components (Table S2). Fe K-edge EXAFS LCF were performed using Schwertmannite (Schw;
 216 As(III)-sorbed and As-free) and AFA as fitting components (Table S3). The sum of the LCF components are normalized to 100%. The uncertainties on the reported values refer
 217 to the last digit and are given under brackets. Uncertainties on biomass values are calculated from the three sample replicates. Uncertainties on XANES and EXAFS LCF
 218 components correspond to 3 times the standard deviation given by the Athena fitting software. Uncertainty calculation method for XANES data is presented in Resongles et al.²⁵.

219 3.3. Microbiological characterization of feed water and biogenic precipitates

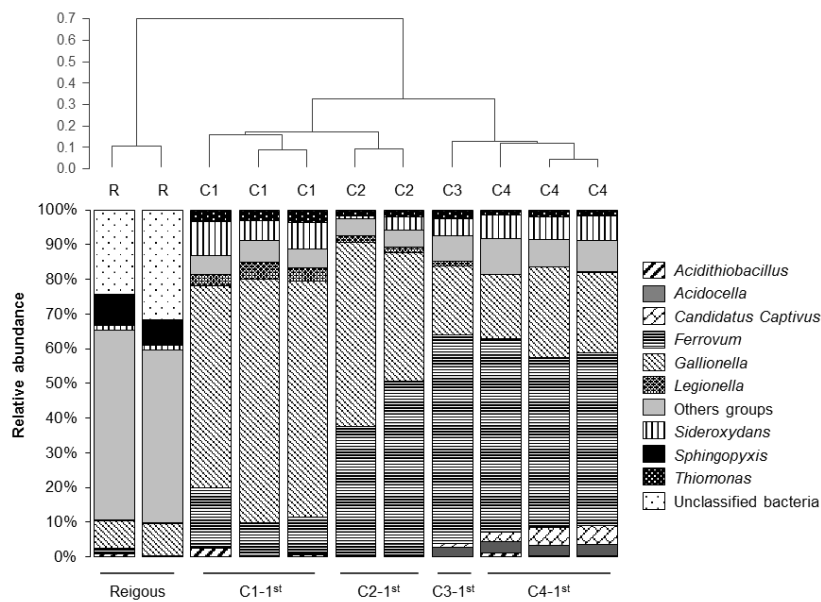
220 3.3.1. *Bacterial cell concentration*

221 Feed water collected from the source of the Reigous Creek contained 5×10^5 bacterial
222 cells mL^{-1} . In the biogenic precipitate, the average bacterial cell concentration was $2 \pm$
223 1×10^7 bacterial cells g^{-1} (dry wt.), without significant differences between the HRT
224 (Table 1).

225 3.3.2. *Bacterial diversity*

226 High-throughput sequencing yielded a total of 429 004 sequences of 16S rRNA gene
227 corresponding to 26 000 quality sequences per sample, which adequately covered the
228 bacterial diversity in all the experiments (Figure S3). Bacterial communities developed
229 in the biogenic precipitates exhibited lower levels of diversity compared to those from
230 the feed water, as evidenced by lower diversity indexes (richness, evenness and
231 Shannon) (Table S5). No clear difference was observed between the channels. In
232 agreement with diversity indices, the bacterial composition in the biogenic precipitates
233 was characterized by the dominance of a relative small number of bacterial OTU
234 (Figure 4). The two most important OTU were affiliated with *Ferrovum* and *Gallionella*
235 genera, representing 31 % and 36 % of the whole dataset sequences, respectively. In the
236 feed water, a much higher richness of OTUs was identified (Table S5). The majority of
237 these OTUs represented less than 1 % of the whole dataset each in term of number of
238 sequences, and were thus referred as “other groups”. Unclassified bacteria were the
239 second most abundant group, followed by *Sphingopyxis* and *Gallionella* with a
240 proportion of less than 10 % each.

241 Application of different HRT strongly impacted the bacterial community structure and
 242 composition in the biogenic precipitates (Figure 4). According to the performed
 243 ANOVA tests, increasing HRT resulted in a significant increase of the proportion of
 244 bacteria affiliated to *Ferrovum* genus (from 12 to 51 % of total sequences), *Candidatus*
 245 *Captivus* genus (from 0.1 to 4 % of total sequences) and *Acidocella* genus (from 0.1 to
 246 3% of total sequences). Conversely, significant decrease was observed for the bacteria
 247 affiliated with *Gallionella* (from 65 % to 23 % of total sequences), *Legionella* (from 4
 248 to 0.1 % of total sequences) and *Thiomonas* (from 3 to 2 % of total sequences) genera.
 249 No effect of HRT was observed for the iron-oxidizing bacteria affiliated with
 250 *Acidithiobacillus* and *Sideroxydans* genera.



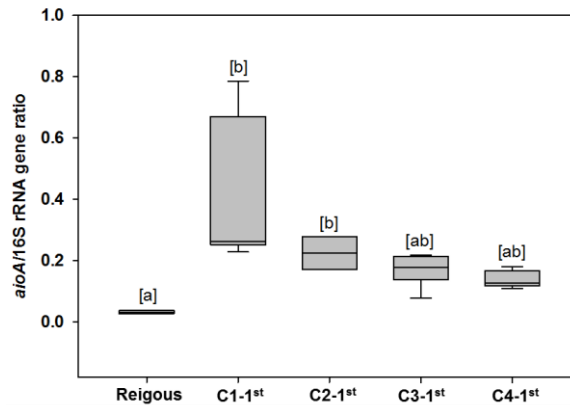
251

252 **Figure 4.** Relative abundance of bacterial genera in Reigous water (R) and in biogenic precipitates
 253 formed in the bottom of the channel under different HRT (C1: 74 min; C2: 130 min; C3: 200 min; C4:
 254 456 min). Cluster tree represents the phylogenetic community distance based on the operational
 255 taxonomic unit (OTU) composition. “Other groups” represent the phylogenetic groups (genus) with a
 256 relative abundance <1 % calculated on the whole dataset.

257

3.3.3. Functional potential of arsenic oxidation

258 The biogenic precipitates exhibited higher *aioA*/16S rRNA gene ratio (average 0.13 to
259 0.40) than the feed water from Reigous Creek (0.03). Difference between HRT was not
260 significant (Figure 5).



261

262 **Figure 5.** *aioA*/16S rRNA gene ratio in the Reigous water and in the biogenic precipitates at the end of
263 the experiment at different HRT. Letters in brackets indicate significant differences between treatments,
264 according to Kruskal-Wallis (p-value < 0.05) and Dunn's multiple comparison tests.

265

4. Discussion

266

4.1. Bioreactor performance and biogenic precipitates composition

267 Increasing the HRT improved the performance of the bioreactor in terms of Fe(II)
268 oxidation and As abatement (Figure 1D). However, performances were lower than in
269 our previous study ¹⁰. Fe(II) oxidation and As removal reached respectively ~50 % and
270 ~40 % for the highest HRT (456 min), whereas in our previous study ¹⁰, these
271 efficiencies were higher than 80 % (Fe(II) oxidation) and 60 % (As removal) at HRT =

272 500 min, in the same operating conditions. The difference may be attributed to higher
273 pH of the AMD water in the present experiment (pH = 3.65) compared to the previous
274 ones (pH = 3.0 to 3.4). In AMD, lower pH promotes fastest rates of biological Fe(II)
275 oxidation, coinciding with the higher Fe(III) solubility²⁸. Furthermore, the lower
276 proportion of As(V) in the feed water (17 %, Table S1) compared to the previous study
277 (As(V) = 17- 39%)¹⁰ did not favor As retention in the biogenic precipitates. Indeed,
278 As(V)-Fe(III) solids forming in AMDs are known to be about ten times less soluble
279 than As(III)-Fe(III) phases²⁶.

280 Increasing the HRT decreased the As/Fe ratio in the biogenic precipitate (Table 1;
281 Figure 3) but did not affect significantly the redox state of arsenic in the solid and the
282 distribution of As-bearing phases. The biogenic precipitates were mainly composed of
283 As(III)-sorbed and As-free schwertmannite, accompanied with minor amounts of
284 As(V)-bearing amorphous ferric arsenate, both phases being typical of AMD systems
285 containing arsenic^{29,30}, including in the Reigous Creek in Carnoulès^{7,31}. Amorphous
286 ferric arsenate has been shown to form in acid sulfate solution with initial dissolved
287 As(V)/Fe(III) molar ratios higher than 0.15–0.2, while As(V)-sorbed schwertmannite
288 formed at lower As(V)/Fe(III) molar ratios^{26,32}. In the present experiments, the
289 dissolved As(V)/Fe(III) molar ratio varied from 0.2 ± 0.1 in the feed water to 0.1 ± 0.1 ,
290 during the oxidation of Fe(II) to Fe(III) in the channels. These ratios are consistent with
291 the presence of amorphous ferric arsenate in the biogenic precipitates. In our
292 experimental pilot system, no tooeleite was detected, whereas this mineral is usually
293 found in Reigous Creek³¹. Maillot *et al.*²⁶ observed the formation of amorphous ferric
294 arsenite at initial dissolved As(III)/Fe(III) molar ratio above 0.6, and As(III)-sorbed
295 schwertmannite below this ratio. Here, the dissolved As(III)/Fe(III) molar ratio varied

296 from 1.0 ± 0.7 in the feed water to 0.5 ± 0.7 , during Fe(II) oxidation. In these
297 conditions, the nucleation of schwertmannite is faster than that of amorphous ferric
298 arsenite or nanocrystalline tooeleite, as shown in the study from Egal *et al.* ³³.

299 **4.2. Influence of the HRT on bacterial communities**

300 **4.2.1. Iron-oxidizing bacteria**

301 The most abundant OTUs found in the biogenic precipitates established at the bottom of
302 the channels were the iron-oxidizing *Betaproteobacteria* related to the *Ferrovum* and
303 *Gallionella* genera. These bacteria have been commonly observed in natural AMD ^{34–36}
304 and in bioreactors for the treatment of acid mine waters ^{37–39}. *Gallionella* dominated the
305 water bacterial community in most of the stations along the Carnoulès AMD whatever
306 the season while *Ferrovum* were less abundant particularly in the upstream more
307 contaminated stations ³⁵.

308 The HRT clearly exerted an effect on bacterial community distribution, especially the
309 relative contribution of *Gallionella* and *Ferrovum*. Several factors can explain this
310 effect. Many studies highlighted pH as the most important factor structuring AMD
311 communities ^{14,15,40}. In our experiment, the outlet pH was lower (2.8) when the highest
312 HRT was applied. Jones *et al.* ³⁶ analyzed the composition of sediment communities
313 from the Red Eyes drainage (USA) and found that *Gallionella*-like organisms were
314 restricted to locations with a pH > 3, whereas *Ferrovum* dominated at pH < 3. Similarly,
315 in a bioreactor for the treatment of acid mine drainage, Heinzl *et al.* ³⁷ reported a shift
316 in the dominant species of the bacterial community from *Ferrovum* relatives to
317 *Gallionella* relatives when the pH increased from 3.0 to 3.4 and the ferric iron
318 concentration decreased from ~105 to ~30 mg L⁻¹. Hallberg ⁴¹ indicated that apart from

319 pH and temperature (constant in our bioreactor), there are more subtle factors such as
320 the affinity for electron acceptors (*e.g.* oxygen), that could drive the structure of the
321 microbial communities. In this respect, *Gallionella* is a microaerophilic bacterium that
322 normally grows at 0.1–1 mg L⁻¹ DO ⁴² while *Ferrovum myxofaciens*, the only species of
323 *Ferrovum* described to date, is a strict aerobe bacterium ⁴³. Such sensitivity to DO
324 concentration might explain the change from *Gallionella* to *Ferrovum* while DO
325 increased from 5 mg L⁻¹ (outlet DO) in C1-74 min (Figure 2) to 7.8 mg L⁻¹ (outlet DO)
326 in C4-456 min. In a similar way, Fabisch *et al.* ⁴⁴ observed that *Ferrovum* increased by
327 10-fold along the flow path of a metal rich mine discharge, presumably due to
328 increasing oxygen content, from 0.8–4.1 mg L⁻¹, in the outflow, to 5.5–9.7 mg L⁻¹ at the
329 most oxygenated site. However, the optimal oxygen conditions of *Ferrovum* sp. have
330 not been well defined yet and some contradictory results have been found ⁴⁵.

331 **4.2.2. Arsenite-oxidizing bacteria**

332 The detection of *aioA* genes and 16S rRNA sequences affiliated with *Thiomonas* spp. in
333 the biogenic precipitates shows that the bacteria having the potential to oxidize arsenic
334 are present in the bioreactor. However, arsenic in the biogenic precipitates was
335 preferentially trapped in the form of As(III) for all the HRT, and outlet water also
336 contained predominantly dissolved As(III) (> 82 %). This suggests that As oxidation
337 was not favored in this experiment. Bacteria belonging to the *Thiomonas* genus were
338 shown to be active *in situ* in the Carnoulès AMD ⁴⁶, and to actively express the enzyme
339 arsenite oxidase although they were not a major member of the bacterial community ⁴⁷.
340 They were also able to oxidize arsenic under laboratory conditions ^{48,49}. The apparent
341 lack of expression of As(III) oxidizing activity in the present experiment remains

342 unexplained. The regulation of the expression of arsenite oxidation genetic potential
343 among *Thiomonas* strains appears to be complex and is not fully understood.

344 The As-oxidizing activity of *Thiomonas* may be modulated by the physico-chemistry of
345 the AMD. In the present study, the original AMD pH was 4.7 but decreased to 3.65
346 under laboratory storage. The growth rate of the arsenite-oxidizing '*Thiomonas*
347 *arsenivorans*' was reduced to half as the starting pH decreased from 4.0 to ~3.5 in batch
348 cultures on a synthetic medium containing 100 mg L⁻¹ As(III)⁵⁰. In similar experiments,
349 Battaglia-Brunet *et al.*⁵¹ observed that the arsenite oxidation rate of the consortium
350 CAsO₁, which contained '*Thiomonas arsenivorans*', decreased (from ~2.15 to ~1.65
351 mg L⁻¹ h⁻¹) with pH change from 4 to 3, and even further at pH 2 (< 0.25 mg L⁻¹ h⁻¹).
352 The bacterial growth followed the same trend. The pH decrease in the feed water under
353 laboratory storage, regardless the HRT, is a potential reason for the lack of As
354 oxidation. However, identification of the regulation factors deserves further research.

355 **4.2.3. Other bacteria**

356 The proportion of *Acidocella* sp., an iron-reducing heterotrophic acidophilic
357 microorganism, increased with increasing HRT, while the outlet pH decreased from 3.2
358 to 2.8. This trend was opposite to that observed in flow-through bioreactors inoculated
359 with sediments from Brubaker Run, in the Appalachian bituminous coal basin, that
360 showed a decrease of *Acidocella* sp. abundance with decreasing pH from 4.2 to 3.3³⁸.
361 Most probably, the increase of the proportion of *Acidocella* sp. in our study can be
362 linked to increasing Fe(III) concentration with increasing HRT. It can be hypothesized
363 that this bacterium thrives in conditions where precipitation of Fe(III) is limited by low
364 pH values.

365 *Legionella* is a non-iron-oxidizing heterotrophic bacterium that is relatively uncommon
366 in AMD. However, it has been reported in AMD of the Xiang Mountain sulfide mine
367 ^{52,53} and was a dominant member of the bacterial community in a tailings pond from a
368 metal mine ⁵⁴. The presence of this bacterium has been attributed to its association with
369 eukaryotic cells that colonize AMD. Similarly, *Candidatus Captivus* is an
370 endosymbiont of protist cells that has been previously observed in AMD from Iron
371 Mountain ⁵⁵. However, as we did not analyze the eukaryotic community in the present
372 experiment, the higher abundance of *Legionella* and *Candidatus Captivus* at lower and
373 higher HRT, respectively, cannot be related to eukaryotes dynamics.

374 **4.3. Environmental significance**

375 The present study confirmed the capacity of our lab-scale channel bioreactor to
376 immobilize arsenic from AMD. This capacity was ascribed to the ability of
377 autochthonous iron-oxidizing bacteria *Gallionella* and *Ferrovum*, present in the original
378 AMD seed water, to oxidize iron at acid pH. Although HRT influenced the structure
379 and composition of the bacterial community that settled in the bioreactor, these bacteria
380 remained dominant members of the community at all HRT values. Such robustness is a
381 key factor for future field-scale application of this treatment. Nevertheless, long-term
382 monitoring of bacterial community during longer bioreactor operation would be
383 required to confirm this stability. Early results from other flow-through bioreactors
384 treating AMD suggest that despite some changes in the microbial community during
385 long-term operation, the biological Fe(II)-oxidizing performance was maintained ^{38,56},
386 which further demonstrated the reliability of this kind of bioreactor for the oxidation of
387 Fe(II) in AMD treatments.

388 Although arsenic abatement increased substantially with HRT, a maximum of 40 % As
389 removal was reached at HRT of ~500 min, which contrasted with the ~80 % As removal
390 in previous experiments ¹⁰. Contrary to the present study, in these earlier experiments
391 As(III) oxidation occurred within the bioreactor, thus improving As removal efficiency.
392 As discussed previously (Section 4.2.2), the factors that regulate arsenite oxidation
393 activity in our bioreactor remain to be deciphered. The importance of such regulation is
394 also crucial regarding the stability of As-bearing solid phases that form during the
395 treatment. Indeed, the dominant phase in the channel bioreactor was As(III)-bearing
396 schwertmannite, with low proportion of amorphous ferric arsenate. As(III)-bearing
397 schwertmannite is a metastable precursor leading to jarosite or goethite while releasing
398 arsenic in the dissolved phase during aging ⁵⁷. Conversely, ferric arsenate phases were
399 shown to be the most suitable for safe disposal ⁵⁸.

400 **Associated content**

401 Supporting information

402 The supporting information section contains Tables S1-S5 and Figures S1-S3.

403 **Author information**

404 Corresponding author: Corinne Casiot

405 Email: casiot@msem.univ-montp2.fr

406 Phone: +33 4 67 14 33 56

407

408 **Acknowledgements**

409 The authors thank the IngECOST-DMA project (ANR-13-ECOT-0009), the OSU
410 OREME (SO POLLUMINE Observatory, funded since 2009) and the Ecole Doctorale
411 GAIA (PhD fellowship of Lidia Fernandez-Rojo, 2014-2017) for the financial support.
412 We thank Remi Freydier for ICP-MS analysis on the AETE-ISO platform (OSU
413 OREME, University of Montpellier). We thank Christophe Duperray, from the
414 Montpellier RIO Imaging microscopy platform, for his kind assistance in cytometry.
415 Mickaël Charron from BRGM it is gratefully acknowledged for its technical assistance
416 on *aioA* gene quantification. We also thank Luca Olivi from the XAFS beamline at the
417 ELETTRA synchrotron (Trieste, Italy).

418

419 **References**

- 420 (1) Williams, M. Arsenic in mine waters: an international study. *Environ. Geol.*
421 **2001**, *40* (3), 267–278.
- 422 (2) Paikaray, S. Arsenic geochemistry of acid mine drainage. *Mine Water Environ.*
423 **2015**, *34* (2), 181–196.
- 424 (3) Battaglia-Brunet, F.; Itard, Y.; Garrido, F.; Delorme, F.; Crouzet, C.; Greffie, C.;
425 Jouliau, C. A simple biogeochemical process removing arsenic from a mine
426 drainage water. *Geomicrobiol. J.* **2006**, *23* (3–4), 201–211.
- 427 (4) Elbaz-Poulichet, F.; Bruneel, O.; Casiot, C. The Carnoulès mine. Generation of
428 As-rich acid mine drainage, natural attenuation processes and solutions for
429 passive in-situ remediation. In *Difpolmine (Diffuse Pollution From Mining*
430 *Activities)*; 2006.
- 431 (5) Macías, F.; Caraballo, M. A.; Nieto, J. M.; Rötting, T. S.; Ayora, C. Natural
432 pretreatment and passive remediation of highly polluted acid mine drainage. *J.*
433 *Environ. Manage.* **2012**, *104* (0), 93–100.
- 434 (6) Asta, M. P.; Ayora, C.; Román-Ross, G.; Cama, J.; Acero, P.; Gault, A. G.;
435 Charnock, J. M.; Bardelli, F. Natural attenuation of arsenic in the Tinto Santa
436 Rosa acid stream (Iberian Pyritic Belt, SW Spain): The role of iron precipitates.
437 *Chem. Geol.* **2010**, *271* (1–2), 1–12.
- 438 (7) Egal, M.; Casiot, C.; Morin, G.; Elbaz-Poulichet, F.; Cordier, M.-A.; Bruneel, O.
439 An updated insight into the natural attenuation of As concentrations in Reigous
440 Creek (southern France). *Appl. Geochemistry* **2010**, *25* (12), 1949–1957.

- 441 (8) Ohnuki, T.; Sakamoto, F.; Kozai, N.; Ozaki, T.; Yoshida, T.; Narumi, I.; Wakai,
442 E.; Sakai, T.; Francis, A. J. Mechanisms of arsenic immobilization in a biomat
443 from mine discharge water. *Chem. Geol.* **2004**, *212* (3–4), 279–290.
- 444 (9) Modis, K.; Adam, K.; Panagopoulos, K.; Kontopoulos, A. Development and
445 Validation of a geostatistical model for prediction of acid mine drainage in
446 underground sulphide mines. In *Transactions - Institution of Mining and*
447 *Metallurgy. Section A. Mining Industry*; Institution of Mining & Metallurgy,
448 1998; Vol. 107, pp A102–A107.
- 449 (10) Fernandez-Rojo, L.; Héry, M.; Le Pape, P.; Braungardt, C.; Desoeuvre, A.;
450 Torres, E.; Tardy, V.; Resongles, E.; Laroche, E.; Delpoux, S.; et al. Biological
451 attenuation of arsenic and iron in a continuous flow bioreactor treating acid mine
452 drainage (AMD). *Water Res.* **2017**, *123*, 594–606.
- 453 (11) Vasquez, Y.; Escobar, M. C.; Neculita, C. M.; Arbeli, Z.; Roldan, F. Biochemical
454 passive reactors for treatment of acid mine drainage: Effect of hydraulic retention
455 time on changes in efficiency, composition of reactive mixture, and microbial
456 activity. *Chemosphere* **2016**, *153*, 244–253.
- 457 (12) Vasquez, Y.; Escobar, M. C.; Saenz, J. S.; Quiceno-Vallejo, M. F.; Neculita, C.
458 M.; Arbeli, Z.; Roldan, F. Effect of hydraulic retention time on microbial
459 community in biochemical passive reactors during treatment of acid mine
460 drainage. *Bioresour. Technol.* **2018**, *247* (4), 624–632.
- 461 (13) Lear, G.; Niyogi, D.; Harding, J.; Dong, Y.; Lewis, G. Biofilm bacterial
462 community structure in streams affected by acid mine drainage. *Appl. Environ.*
463 *Microbiol.* **2009**, *75* (11), 3455–3460.

- 464 (14) Kuang, J.-L.; Huang, L.-N.; Chen, L.-X.; Hua, Z.-S.; Li, S.-J.; Hu, M.; Li, J.-T.;
465 Shu, W.-S. Contemporary environmental variation determines microbial diversity
466 patterns in acid mine drainage. *ISME J.* **2013**, *7* (5), 1038–1050.
- 467 (15) Chen, L.; Li, J.; Chen, Y.; Huang, L.; Hua, Z.; Hu, M.; Shu, W. Shifts in
468 microbial community composition and function in the acidification of a lead/zinc
469 mine tailings. *Environ. Microbiol.* **2013**, *15* (9), 2431–2444.
- 470 (16) Edwards, K. J.; Gihring, T. M.; Banfield, J. F. Seasonal variations in microbial
471 populations and environmental conditions in an extreme acid mine drainage
472 environment. *Appl. Environ. Microbiol.* **1999**, *65* (8), 3627–3632.
- 473 (17) González-Toril, E.; Aguilera, A.; Souza-Egipsy, V.; López Pamo, E.; Sánchez
474 España, J.; Amils, R. Geomicrobiology of La Zarza-Perrunal acid mine effluent
475 (Iberian Pyritic Belt, Spain). *Appl. Environ. Microbiol.* **2011**, *77* (8), 2685–2694.
- 476 (18) Cheng, H.; Hu, Y.; Luo, J.; Xu, B.; Zhao, J. Geochemical processes controlling
477 fate and transport of arsenic in acid mine drainage (AMD) and natural systems. *J*
478 *Hazard Mater* **2009**, *165* (1–3), 13–26.
- 479 (19) Barret, M.; Briand, M.; Bonneau, S.; Préveaux, A.; Valière, S.; Bouchez, O.;
480 Hunault, G.; Simoneau, P.; Jacquesa, M.-A. Emergence shapes the structure of
481 the seed microbiota. *Appl. Environ. Microbiol.* **2015**, *81* (4), 1257–1266.
- 482 (20) Wang, Y.; Qian, P.-Y. Conservative fragments in bacterial 16S rRNA genes and
483 primer design for 16S ribosomal DNA amplicons in metagenomic studies. *PLoS*
484 *One* **2009**, *4* (10), e7401.
- 485 (21) Schloss, P. D.; Westcott, S. L.; Ryabin, T.; Hall, J. R.; Hartmann, M.; Hollister,

- 486 E. B.; Lesniewski, R. A.; Oakley, B. B.; Parks, D. H.; Robinson, C. J.; et al.
487 Introducing mothur: Open-source, platform-independent, community-supported
488 software for describing and comparing microbial communities. *Appl. Environ.*
489 *Microbiol.* **2009**, 75 (23), 7537–7541.
- 490 (22) Wang, Q.; Garrity, G. M.; Tiedje, J. M.; Cole, J. R. Naive Bayesian classifier for
491 rapid assignment of rRNA sequences into the new bacterial taxonomy. *Appl.*
492 *Environ. Microbiol.* **2007**, 73 (16), 5261–5267.
- 493 (23) Tardy, V.; Casiot, C.; Fernandez-Rojo, L.; Resongles, E.; Desoeuvre, A.; Joulian,
494 C.; Battaglia-Brunet, F.; Héry, M. Temperature and nutrients as drivers of
495 microbially mediated arsenic oxidation and removal from acid mine drainage.
496 *Appl. Microbiol. Biotechnol.* **2018**, 1–12.
- 497 (24) Ravel, B.; Newville, M. *ATHENA*, *ARTEMIS*, *HEPHAESTUS*: data analysis for
498 X-ray absorption spectroscopy using *IFEFFIT*. *J. Synchrotron Radiat.* **2005**, 12
499 (4), 537–541.
- 500 (25) Resongles, E.; Le Pape, P.; Fernandez-Rojo, L.; Morin, G.; Brest, J.; Guo, S.;
501 Casiot, C. Routine determination of inorganic arsenic speciation in precipitates
502 from acid mine drainage using orthophosphoric acid extraction followed by
503 HPLC-ICP-MS. *Anal. Methods* **2016**, 8, 7420–7426.
- 504 (26) Maillot, F.; Morin, G.; Juillot, F.; Bruneel, O.; Casiot, C.; Ona-Nguema, G.;
505 Wang, Y.; Lebrun, S.; Aubry, E.; Vlaic, G.; et al. Structure and reactivity of
506 As(III)- and As(V)-rich schwertmannites and amorphous ferric arsenate sulfate
507 from the Carnoulès acid mine drainage, France: Comparison with biotic and
508 abiotic model compounds and implications for As remediation. *Geochim.*

- 509 *Cosmochim. Acta* **2013**, *104*, 310–329.
- 510 (27) Casiot, C.; Morin, G.; Juillot, F.; Bruneel, O.; Personné, J.-C.; Leblanc, M.;
511 Duquesne, K.; Bonnefoy, V.; Elbaz-Poulichet, F. Bacterial immobilization and
512 oxidation of arsenic in acid mine drainage (Carnoulès creek, France). *Water Res.*
513 **2003**, *37* (12), 2929–2936.
- 514 (28) Larson, L. N.; Sánchez-España, J.; Kaley, B.; Sheng, Y.; Bibby, K.; Burgos, W.
515 D. Thermodynamic controls on the kinetics of microbial low-pH Fe(II) oxidation.
516 *Environ. Sci. Technol.* **2014**, *48* (16), 9246–9254.
- 517 (29) Fukushi, K.; Sasaki, M.; Sato, T.; Yanase, N.; Amano, H.; Ikeda, H. A natural
518 attenuation of arsenic in drainage from an abandoned arsenic mine dump. *Appl.*
519 *Geochemistry* **2003**, *18* (8), 1267–1278.
- 520 (30) Courtin-Nomade, A.; Grosbois, C.; Bril, H.; Roussel, C. Spatial variability of
521 arsenic in some iron-rich deposits generated by acid mine drainage. *Appl.*
522 *Geochemistry* **2005**, *20* (2), 383–396.
- 523 (31) Morin, G.; Juillot, F.; Casiot, C.; Bruneel, O.; Personné, J.-C.; Elbaz-Poulichet,
524 F.; Leblanc, M.; Ildefonse, P.; Calas, G. Bacterial formation of tooeleite and
525 mixed arsenic(III) or arsenic(V)–iron(III) gels in the Carnoulès acid mine
526 drainage, France. A XANES, XRD, and SEM study. *Environ. Sci. Technol.* **2003**,
527 *37* (9), 1705–1712.
- 528 (32) Carlson, L.; Bigham, J. M.; Schwertmann, U.; Kyek, A.; Wagner, F. Scavenging
529 of As from acid mine drainage by schwertmannite and ferrihydrite: a comparison
530 with synthetic analogues. *Env. Sci Technol* **2002**, *36* (8), 1712–1719.

- 531 (33) Egal, M.; Casiot, C.; Morin, G.; Parmentier, M.; Bruneel, O.; Lebrun, S.; Elbaz-
532 Poulichet, F. Kinetic control on the formation of tooeleite, schwertmannite and
533 jarosite by *Acidithiobacillus ferrooxidans* strains in an As(III)-rich acid mine
534 water. *Chem. Geol.* **2009**, *265* (3–4), 432–441.
- 535 (34) Kimura, S.; Bryan, C. G.; Hallberg, K. B.; Johnson, D. B. Biodiversity and
536 geochemistry of an extremely acidic, low-temperature subterranean environment
537 sustained by chemolithotrophy. *Environ. Microbiol.* **2011**, *13* (8), 2092–2104.
- 538 (35) Volant, A.; Bruneel, O.; Desoeuvre, A.; Héry, M.; Casiot, C.; Bru, N.; Delpoux,
539 S.; Fahy, A.; Javerliat, F.; Bouchez, O.; et al. Diversity and spatiotemporal
540 dynamics of bacterial communities: physicochemical and other drivers along an
541 acid mine drainage. *FEMS Microbiol. Ecol.* **2014**, *90* (1), 247–263.
- 542 (36) Jones, D. S.; Kohl, C.; Grettenberger, C.; Larson, L. N.; Burgos, W. D.;
543 Macaladya, J. L. Geochemical niches of iron-oxidizing acidophiles in acidic coal
544 mine drainage. *Appl. Environ. Microbiol.* **2015**, *81* (4), 1242–1250.
- 545 (37) Heinzl, E.; Janneck, E.; Glombitza, F.; Schlömann, M.; Seifert, J. Population
546 dynamics of iron-oxidizing communities in pilot plants for the treatment of acid
547 mine waters. *Environ. Sci. Technol.* **2009**, *43* (16), 6138–6144.
- 548 (38) Sheng, Y.; Bibby, K.; Grettenberger, C.; Kaley, B.; Macalady, J. L.; Wang, G.;
549 Burgos, W. D. Geochemical and temporal influences on the enrichment of
550 acidophilic iron-oxidizing bacterial communities. *Appl. Environ. Microbiol.*
551 **2016**, *82* (12), 3611–3621.
- 552 (39) Sun, W.; Xiao, E.; Kalin, M.; Krumins, V.; Dong, Y.; Ning, Z.; Liu, T.; Sun, M.;

- 553 Zhao, Y.; Wu, S.; et al. Remediation of antimony-rich mine waters: Assessment
554 of antimony removal and shifts in the microbial community of an onsite field-
555 scale bioreactor. *Environ. Pollut.* **2016**, *215*, 213–222.
- 556 (40) Teng, W.; Kuang, J.; Luo, Z.; Shu, W. Microbial diversity and community
557 assembly across environmental gradients in acid mine drainage. *Minerals* **2017**, *7*
558 (6), 106.
- 559 (41) Hallberg, K. B. New perspectives in acid mine drainage microbiology.
560 *Hydrometallurgy* **2010**, *104* (3–4), 448–453.
- 561 (42) Hanert, H. H. The genus *Gallionella*. In *The Prokaryotes*; Springer New York:
562 New York, NY, 2006; pp 990–995.
- 563 (43) Johnson, D. B.; Hallberg, K. B.; Hedrich, S. Uncovering a microbial enigma:
564 isolation and characterization of the streamer-generating, iron-oxidizing,
565 acidophilic bacterium *Ferrovum myxofaciens*. *Appl. Environ. Microbiol.* **2014**, *80*
566 (2), 672–680.
- 567 (44) Fabisch, M.; Freyer, G.; Johnson, C. A.; Büchel, G.; Akob, D. M.; Neu, T. R.;
568 Küsel, K. Dominance of “*Gallionella capsiferiformans*” and heavy metal
569 association with *Gallionella*-like stalks in metal-rich pH 6 mine water discharge.
570 *Geobiology* **2016**, *14* (1), 68–90.
- 571 (45) Jwair, R. J.; Tischler, J. S.; Janneck, E.; Schlömann, M. Acid mine water
572 treatment using novel acidophilic iron-oxidizing bacteria of the genus
573 “*Ferrovum*”: effect of oxygen and carbon dioxide on survival. In *Mining Meets*
574 *Water – Conflicts and Solutions*; Drebenstedt, C., Paul, M., Eds.; 2016; pp 1060–

- 575 1063.
- 576 (46) Bruneel, O.; Volant, A.; Gallien, S.; Chaumande, B.; Casiot, C.; Carapito, C.;
577 Bardil, A.; Morin, G.; Brown Jr., G. E.; Personné, J. C.; et al. Characterization of
578 the active bacterial community involved in natural attenuation processes in
579 arsenic-rich creek sediments. *Microb Ecol* **2011**, *61* (4), 793–810.
- 580 (47) Hovasse, A.; Bruneel, O.; Casiot, C.; Desoeuvre, A.; Farasin, J.; Hery, M.; Van
581 Dorsselaer, A.; Carapito, C.; Arsène-Ploetze, F. Spatio-temporal detection of the
582 *Thiomonas* population and the *Thiomonas* arsenite oxidase involved in natural
583 arsenite attenuation processes in the Carnoulès acid mine drainage. *Front. cell*
584 *Dev. Biol.* **2016**, *4* (3), 1–14.
- 585 (48) Bruneel, O.; Personné, J. C.; Casiot, C.; Leblanc, M.; Elbaz-Poulichet, F.;
586 Mahler, B. J.; Le Flèche, A.; Grimont, P. A. D. Mediation of arsenic oxidation by
587 *Thiomonas* sp. in acid-mine drainage (Carnoulès, France). *J. Appl. Microbiol.*
588 **2003**, *95* (3), 492–499.
- 589 (49) Duquesne, K.; Lieutaud, A.; Ratouchniak, J.; Muller, D.; Lett, M.-C.; Bonnefoy,
590 V. Arsenite oxidation by a chemoautotrophic moderately acidophilic *Thiomonas*
591 sp.: from the strain isolation to the gene study. *Environ. Microbiol.* **2008**, *10* (1),
592 228–237.
- 593 (50) Battaglia-Brunet, F.; Joulain, C.; Garrido, F.; Dictor, M.-C.; Morin, D.;
594 Coupland, K.; Barrie Johnson, D.; Hallberg, K. B.; Baranger, P. Oxidation of
595 arsenite by *Thiomonas* strains and characterization of *Thiomonas arsenivorans*
596 sp. nov. *Antonie Van Leeuwenhoek* **2006**, *89* (1), 99–108.

- 597 (51) Battaglia-Brunet, F.; Dictor, M.-C.; Garrido, F.; Crouzet, C.; Morin, D.;
598 Dekeyser, K.; Clarens, M.; Baranger, P. An arsenic(III)-oxidizing bacterial
599 population: selection, characterization, and performance in reactors. *J. Appl.*
600 *Microbiol.* **2002**, *93* (4), 656–667.
- 601 (52) Hao, C.; Wang, L.; Gao, Y.; Zhang, L.; Dong, H. Microbial diversity in acid
602 mine drainage of Xiang Mountain sulfide mine, Anhui Province, China.
603 *Extremophiles* **2010**, *14* (5), 465–474.
- 604 (53) Hao, C.; Zhang, L.; Wang, L.; Li, S.; Dong, H. Microbial community
605 composition in acid mine drainage lake of Xiang Mountain sulfide mine in Anhui
606 province, China. *Geomicrobiol. J.* **2012**, *29* (10), 886–895.
- 607 (54) Auld, R. R.; Myre, M.; Mykytczuk, N. C. S.; Leduc, L. G.; Merritt, T. J. S.
608 Characterization of the microbial acid mine drainage microbial community using
609 culturing and direct sequencing techniques. *J. Microbiol. Methods* **2013**, *93* (2),
610 108–115.
- 611 (55) Baker, B. J.; Hugenholtz, P.; Dawson, S. C.; Banfield, J. F. Extremely acidophilic
612 protists from acid mine drainage host *Rickettsiales*-lineage endosymbionts that
613 have intervening sequences in their 16S rRNA genes. *Appl. Environ. Microbiol.*
614 **2003**, *69* (9), 5512–5518.
- 615 (56) Jones, R. M.; Johnson, D. B. Iron kinetics and evolution of microbial populations
616 in low-pH, ferrous iron-oxidizing bioreactors. **2016**.
- 617 (57) Acero, P.; Ayora, C.; Torrentó, C.; Nieto, J.-M. The behavior of trace elements
618 during schwertmannite precipitation and subsequent transformation into goethite

- 619 and jarosite. *Geochim. Cosmochim. Acta* **2006**, *70* (16), 4130–4139.
- 620 (58) Lawrence, R. W.; Higgs, S. A. T. W. Removing and stabilizing As in acid mine
621 water. *JOM* **1999**, *51* (9), 27–29.
- 622